A First-Principles Computation of the Low-Energy Polymorphic Forms of the Acetic Acid Crystal. A Test of the Atom−Atom Force Field Predictions

Carme Rovira* and Juan J. Novoa*

Departament Química Física and CER Química Teórica, Fac. Química, University of Barcelona, Av. Diagonal 647, 08028-Barcelona, Spain

Received: June 16, 2000; In Final Form: November 3, 2000

The energetics and structure of the lowest-energy polymorphic forms of the acetic acid crystal previously found by using the UPACK polymorph predictor program and standard atom−atom potentials (GROMOS) has been evaluated by a first-principles Car−Parrinello molecular dynamics method, which takes into account the periodic conditions of the solids within the framework of density functional (DFT) methodology. Our results show that one has to include a correction on the DFT energy to reproduce the experimental value of the interaction energy of the crystal, although this correction does not change the relative energetic ordering of the most stable polymorphic forms. It is also found that the most stable form in these ab initio computations is the UPACK/GROMOS structure closest to the experimental one (polymorph 13), which ranked 15th in the UPACK/GROMOS computations. The crystal structures obtained by the UPACK/GROMOS are qualitatively sounding, but they are too densely packed when compared to the experimental structure. Due to this fact, the DFT interaction energy of these forms is much weaker than that computed for the experimental structure. Due to this, when the UPACK/GROMOS structure of polymorph 13 is fully optimized at the ab initio level, it expands and transforms without barrier to the low-pressure experimental structure. A short-time ab initio dynamics simulation at 150 K on that relaxed structure did not show the presence of phase transformation toward another polymorphic structure. A similar trend is found for the high-pressure polymorph.

Introduction

The study of polymorphism[1] is a very challenging subject with important influence in various fields of material science because of the well-documented experimental fact that different polymorphic forms of the same chemical compound sometimes present opposite physical properties (for instance, magnetic[2] or conducting[3] properties). Consequently, there has been a serious interest in recent years to develop a methodology capable of predicting the most suitable polymorphic forms that a chemical compound could adopt when it packs into a crystalline solid.[1,4] As result of such effort, a series of computer programs have been developed, aimed at predicting the energetically most stable polymorphs in which a chemical compound crystallizes. This is done by systematically searching for all minima in the lattice energy space of the crystal structures.[5] The only input information in these programs are the chemical structure of the compound to crystallize and a set of atom−atom force-field parameters capable of properly describing the intermolecular interactions among the molecules which form the polymorphs.[5]

However, the general experience in the application of these programs to the prediction of polymorphic forms is that they systematically predict within a window of around 2 kcal/mol above the energy of the most stable polymorph, many more polymorphs than observed experimentally.[4a,6] Besides, although there are cases in which the global minimum corresponds to the reported experimental structure,[5,7] sometimes the global minimum is so close in energy to polymorphs that there is no reason to select one specific polymorph. Finally, there are cases in which the polymorph resembling more closely the experimental structure ranks high in the order of stability predicted by these programs.[6a] In the last two situations, the polymorphs were properly characterized minimum-energy structures in the force-field employed, and their absolute energy was in the range of the experimental value, when available.[4]

Besides the previous problems in the relative energy scale, there is another potential drawback in some predicted polymorphs not always addressed, the quality of the geometrical structures predicted. Some studies have concluded that the force field employed in the computations do not seem to strongly affect the main features of the crystal structure.[6] However, in some cases, there are important differences between the experimental structure and the computed geometry closest to the experimental one.[6,8] These differences are manifested when looking at the geometry of the shortest contacts or at the distribution of the geometrical parameter values for these contacts, which do not follow the trends found in statistical studies of experimental crystals. In other cases, as in the low-pressure acetic acid crystal,[6] the differences between computed and experimental structures are even manifested in the crystallographic cell parameters. These geometrical and energetical discrepancies are indications of possible error compensations, or even of lack of quality of the atom−atom potentials employed in the theoretical prediction of the polymorphic structures, a possibility already pointed out in the literature.[9]

In light of the previous considerations, we decided to carry out a systematic evaluation, using Car−Parrinello density functional (DFT) ab initio methods, on the energetic and geometrical quality of the polymorphs predicted by the currently available atom−atom potentials. We will perform this test on the recently reported polymorphs of acetic acid,[6] a complete and detailed theoretical study using various state-of-the-art

* Corresponding authors. E-mail: novoa@qf.ub.es

10.1021/jp0021704 CCC: $20.00
Published on Web 02/07/2001

atom−atom force fields. In particular, we will focus our attention into the structures obtained using the UPACK polymorph predictor package and the GROMOS force-field.[6a] We will fist look at the energetics of the most stable of these UPACK-GROMOS polymorphs and compare it with that obtained with the Car−Parrinello DFT methodology. We will show that while the structure resembling most closely the experimental crystal (polymorph 13) ranks 15th with the GROMOS empirical potentials, at the ab initio level is the one lowest in energy. The ab initio interaction energy for polymorph 13 is much higher than that computed for the experimental structure with the same methodology. We will show that this is due to the overcompression of polymorph 13 with respect to the experimental structure; an ab initio geometry optimization of the UPACK/GROMOS optimized structure of polymorph 13 shows that this structure relaxes without barrier into the experimental structure, thus recovering the above-mentioned energy difference. However, as we will show, the obtention of interaction energies close to the experimental values for these polymorphs is only possible when the total energy computed with the density functional is corrected by a term aimed at compensating for the underestimation introduced by these functional methods on the interaction energy of weak intermolecular bonds. The analysis of the nature of this correction term on model dimers allows us to call it dispersion. This term will be shown to have no influence on the relative stability of the most stable polymorphs. The previous results are all obtained at 0 K. We will also show, by a short-time dynamics simulation at 150 K, that the optimum ab initio structure for the most stable polymorph does not present a phase transformation toward another polymorphic structure during the time of the dynamics, and the parameters remain close to the optimum 0 K values. In conclusion, these results show that some of the problems detected on the atom−atom computed structures disappear when the energy and geometry of these polymorphic structures are computed at the ab initio level.

TABLE 1: Structures Included in the Subset of the 30 Most Stable Polymorphs Computed Using the UPACK Program and the GROMOS Force Field[a]

number	sp group	motif	GROMOS energy[b]
715	*C*2/*c*	cat-e	0.
494	*P*21/*c*	cat-h	0.04
9	*P*212121	cat-h	0.1
14	*P*21	cat-h	0.1
119	*P*21/*c*	cat-h	0.1
76	*Pna*21	cat-h	0.1
45	*P*21/*c*	cat-e	0.1
4	*Pbca*	cat-e	0.1
13′	*C*2/*c*	cat-e	0.1
125	*P*-1	ring	0.1
362	*P*21/*c*	cat-e	0.1
116	*P*21/*c*	ring	0.2
815	*P*21/*c*	cat-h	0.2
31	*P*21/*c*	ring	0.2
13	*Pna*21	cat-e	0.3
50	*P*21/*c*	ring	0.3
118	*P*-1	ring	0.3
930	*C*2/*c*	cat-e	0.3
34	*P*21/*c*	ring	0.3
216	*P*21/*c*	cat-e	0.3
973	*P*21/*c*	ring	0.4
97	*P*212121	cat-e	0.4
16	*C*2/*c*	ring	0.4
181	*P*21/*c*	cat-s	0.4
41	*P*21	cat-e	0.4
6	*Pbca*	cat-e	0.4
976	*C*2/*c*	ring	0.4
28	*P*212121	cat-e	0.4
1002	*P*21/*c*	cat-e	0.4
219	*P*21/*c*	ring	0.5

[a] Each structure is identified by an identification number (first column) identical to that given to it in ref 6, the space group, the main packing motif (see text and Figure 1 for definitions), and the interaction energy (in kcal/mol) computed using the GROMOS force-field. [b] The GROMOS total energy is −16.72 kcal/mol plus the value given in this column.

Computational Details

Acetic acid is a good test model for studying the polymorphism of carboxylic acids. Consequently, it has been the focus of many theoretical studies aimed at understanding its preference for the catemer packing motif.[6,10−12] Only one crystal form is known at low pressures, presenting a catemer packing motif, in clear contraposition with other carboxylic acids which pack forming cyclic dimers.[10] Recently a high-pressure polymorphic form of the acetic acid has also been determined experimentally by ab initio computations.[11] Its packing also presents a catemer packing motif. This preference for the catemer motif of the acetic acid has been the subject of various theoretical studies, carried out using aggregates of acetic acid molecules in the gas phase or in solution.[12]

On the other hand, using some of the available crystal polymorph predictor programs[3] and atom−atom force fields, one can find valuable information on the most stable polymorphic forms of the acetic acid crystals.[6] These studies show that both the catemer and ring motifs are possible minimum-energy structures, with a small energy difference between these two forms. However, the structure (polymorph 13) most closely resembling the low-pressure experimental one ranks 15th, 0.3 kcal/mol above the energy of their most stable polymorph, structure 715. However, as shown in Figure 1, although the qualitative features of the packing are well reproduced, its structure presents non-negligible differences with the experimental neutron diffraction structure: the *c* axis is much shorter, while the *a* axis is a bit larger, the overall effect being an overcompression of the molecules, manifested in the shorter intermolecular contacts between the two chains running along the *c* axis (the contacts at 2.670 and 3.570 Å are shifted to 2.439 and 3.089 Å) or in the contacts within the chains (the contact at 1.642 Å shifts up to 1.596 Å).

We decided to compare the interaction energy and geometry for the lowest-energy polymorphs predicted in the UPACK/GROMOS study[6a] with those obtained from ab initio computations. The ab initio method employed in these studies is a Becke−Perdew nonlocal exchange-correlation DFT formulation of a Car−Parrinello molecular dynamics method,[13] implemented in a Car−Parrinello code capable of doing periodic structure calculations.[14] Other functionals we tested gave nearly the same order of relative energies, and consequently, we will not further discuss their results. For such evaluation, we selected those UPACK/GROMOS polymorphs lying within a 1.2 kcal/mol energy window above the most stable of these structures (polymorph 715). From these structures, we built two subsets: the first subset includes the 30 most stable UPACK-GROMOS optimized structures, without paying attention at their space group (they all have UPACK/GROMOS energies within a 0.5 kcal/mol energy window from the lowest energy); the second subset was built with the eight lowest-energy structures of *Pna*21 symmetry, the space group to which belongs the experimental low-pressure acetic acid crystal. Tables 1 and 2 show the main features of these two subsets (note that structures number 13 and 76 are found in both tables). The unit cell parameters and fractional coordinates employed in this study are those given as Supplementary Material in ref 6a. We identified the poly-

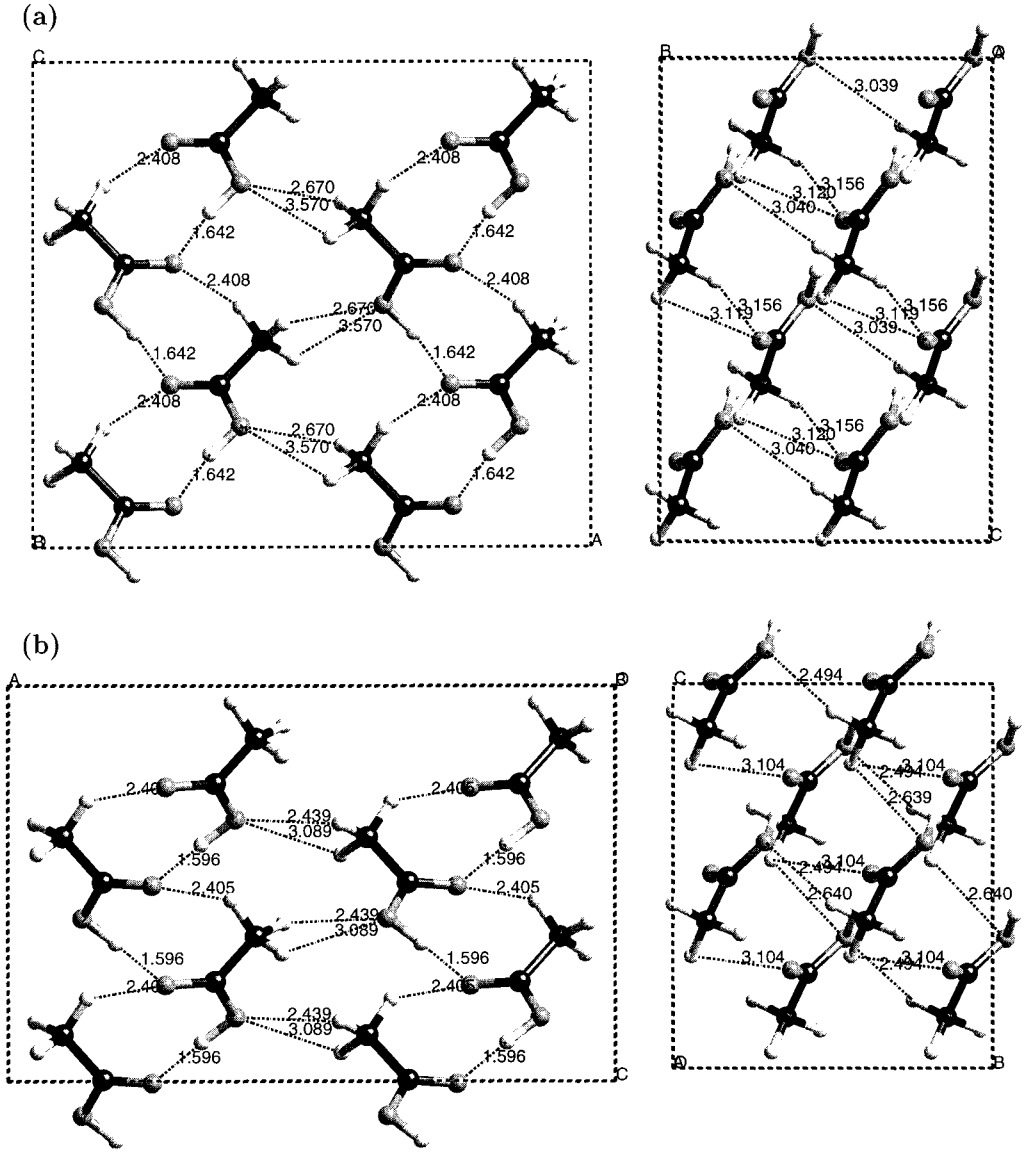

Figure 1. (a) Views of the structure of the low-pressure experimental acetic acid crystal (neutron diffraction). (b) Views of the UPACK/GROMOS polymorph which more closely resembles the low-pressure experimental structure (polymorph 13, see text).

TABLE 2: Structures Included in the Subset of the Eight Most Stable UPACK-GROMOS Polymorphs Presenting *Pna*21 Spatial Group Symmetry[a]

number	motif	GROMOS energy[b]
76	cat-h	0.1
13	cat-e	0.3
34	cat-e	0.6
47	cat-h	0.7
78	cat-h	0.7
63	cat-e	0.7
182	cat-OH	1.0
79	cat-OH	1.3

[a] For each structure, we report its identification number in this work, its reference number given in reference 6, its main packing motif found in the crystal (see text and Figure 1 for definitions), and its interaction energy (in kcal/mol) computed using the GROMOS force-field. [b] The GROMOS total energy is −16.72 kcal/mol plus the value given in this column.

morphic forms according to the same numbering scheme employed in reference 6a.

The Car−Parrinello computations were done using the CPMD program, version 3.0.[15] In this program, the Kohn−Sham orbitals are expanded in a plane wave (PW) basis up to a kinetic energy cutoff of 70 Rydbergs (which corresponds to approximately 36000 PW's per orbital). The atoms are described by ab initio Troullier−Martins pseudopotentials.[16] Additional calculations were performed to verify that the energy was converged relative to the use of larger PW cutoffs (in PW computations this is equivalent to investigating the basis set convergence). The use of PW expansions fully avoids the presence of basis set superposition errors in our computations. We numerically verified this fact by comparing the interaction energy obtained from CPMD calculations on isolated acetic acid dimers and the interaction energy for the same isolated dimer computed by Gaussian-98 when using the BP86 nonlocal exchange-correlation functional, the 6-311++G(2d,2p) atomic Gaussian basis set, and correcting the interaction energy by the basis set superposition error.[17] We used only the Γ point of the Brillouin zone and supercells made of four or six unit cells to compensate for this fact. In selected cases, we verified that this supercell gives total energies very similar to those obtained with larger supercells. Furthermore, the relative energies computed in this way by the CPMD program were found to be qualitatively similar to those obtained with CRYSTAL[18] using about 20

k-points in the Brillouin zone and the 6-31G(2d,2p) atomic basis set. Once the total energy of the crystal is known, the interaction energy per molecule for a molecule in the crystal was computed by subtracting that total energy (of the *n* molecules of the crystal supercell) from the sum of the energies of the n isolated molecules in the cell. Molecular dynamics simulation at finite temperature used an integration step of 0.12 fs, the fictious mass of the electrons was set to 700 au, and the deuteron mass was used for all hydrogen atoms. After an initial equilibration time of 1 ps, the dynamics were continued for a variable time length. Variable-cell molecular dynamics were performed using the Parrinello−Rahman method, as implemented in the CPMD code, using a cutoff of 100 Rydbergs. The CPMD computations were carried out on the SGI-2000 of CEPBA, using up to eight processors, and 1 Gb of central memory.

It is well-known that density functional (DFT) methods do not properly reproduce the dispersion contribution of the interaction energy[19] and predict weaker intermolecular complexes than found experimentally. This is specially important for systems in which the dispersion contribution is an important part of the interaction energy, like in van der Waals or C−H···O hydrogen bonded complexes.[19] Therefore, given the presence of many short C−H···O contacts in the acetic acid polymorphs, we decided to complement the total interaction energy obtained from the Becke−Perdew (BP) computations with an empirical correction term. This correction term is of the form $-(^1/_2)C_iC_j/R_{ij}^6$ and will be added according to the degree of error between the DFT and MP2 interaction energies for each type of intermolecular bond found in the crystal. A similar approach has already found to give good results on the crystals of acetylene[20] and benzene.[21] Such a term will be added on all intermolecular atom−atom interactions whose distance is larger than 2.5 Å and shorter than 12 Å. Extending the value of the cutoff to values larger than 12 Å did not change the size of the dispersion correction on the tested polymorphs. We will show below, on model dimer computations, that the BP computations give interaction energies closer to the Hartree−Fock (HF) than to those given by methods which properly account for the electronic correlation found in hydrogen bonded dimers, like the second-order Moller−Plesset (MP2) method. As most of the MP2−HF energy difference is usually assigned to the dispersion component (the correlation also affects the charge distribution and polarizability, thus forcing a change in the electrostatic and polarization components), we can also call the empirical correction the "dispersion term". Therefore, in the remainder of this paper, we will call the uncorrected and corrected interaction energies BP and BP-disp, respectively. The C_i coefficients of the correction term were taken from those previously proposed in the literature for carboxylic acids.[12a] We will perform MP2 computations on model dimers and small aggregates of the acetic acid to calibrate the quality of the BP and BP-disp potential energy curves. Such computations will be carried out using the Gaussian-98 code[22] and the 6-311++G-(2d,2p) basis set on representative model dimer geometries described below.

It is interesting to point some facts on the main characteristics of the two subsets selected for their study. First of all, a large variety of space groups is found in the first subset, the most frequent being the *P*21/*c* group, followed by the *C*2/*c*, *Pna*21, *P*-1, and *P*212121 groups. It is also worth mentioning the variety of packing motifs: an analysis of their packing shows the presence of the four packing motifs displayed in Figure 2, which we will hereafter identify as the catemer-experimental (cat-e), catemer-helicoidal (cat-h), catemer-OH (cat-OH), and ring (ring) motifs. The main packing motif present in each crystal is also collected in Tables 1 and 2. The most frequent motif is the catemer-experimental motif, found in 15 structures, followed by the ring (10 structures), catemer-helicoidal (9 structures), and catemer-OH (2 structures) motifs. Note also the variety of packing motifs found within the same space group. For instance, in the crystals of the *Pna*21 group one finds three different types of packing motifs (all except the ring motif). All these facts are an indication of the variety of polymorphic structures sampled by the currently available polymorph predictor programs.

Results and Discussion

Accuracy of the DFT Computed Interaction Energies in Acetic Acid Crystals. The experimental interaction energy per molecule for the neutron diffraction low-pressure experimental structure of the acetic acid[23] lies in the −16 to −17 kcal/mol range. The BP value obtained at the conditions specified in the Computational Details section is −7.32 kcal/mol, consistent will the above-mentioned tendency of the DFT functionals to give interaction energies smaller than the experimental results. Therefore, we have to add a properly chosen correction term to compensate for this difference.

The analysis of the low-pressure experimental structure of acetic acid and the most stable UPACK/GROMOS polymorphs indicates the presence of three types of intermolecular bonds: O−H···O═C, C−H···OH, and C−H···O═C. This can be illustrated on the experimental structure of the acetic acid crystal (Figure 1). It can be described as a primary structure of acetic acid ribbons,[24] in which the molecules form $R_2^2(8)$ patterns[25] involving a O−H···O═C bond and a C−H···O═C bond. The ribbons then aggregate to form a secondary structure of planes[24] by means of C−H···OH and C−H···O═C bonds. Finally, the planes pile up by means of C−H···OH and C−H···O═C bonds (tertiary structure,)[24] with the consecutive planes rotated by 90° relative to each other. To obtain a good quantitative description of the interaction energy of this crystal using a particular method, it is necessary to be able to reproduce the interaction of each type of intermolecular bond with precision. Thus, we can investigate the source of the difference between the BP and experimental interaction energy by evaluating how well the BP method performs in describing the interaction energy of model dimers presenting the three types of intermolecular bonds found in these crystals.

We have estimated the error in the BP interaction energies using the acetic acid dimers of Figure 3. They are oriented in such a way that they allow for reproducing an isolated C−H···OH and C−H···O═C bond (Figures 3a and 3b, respectively) and a combined O−H···O═C and C−H···O═C bond (Figure 3c). We have computed for these three dimers the change of the interaction energy as a function of the intermolecular distance when the interaction energy is computed at the HF, MP2, and BP levels. We have also included in this figure the shape of the curve resulting after correcting the BP curves by the dispersion term (the BP-disp curve). All the values are BSSE-corrected, and the basis set is the 6-311++G(2d,2p) set.

To analyze these curves, it is interesting to keep in mind that a MP2/6-311++G(2d,2p) computational level is known from previous computations to reproduce the interaction energy of weak and strong intermolecular hydrogen bonds with precision.[26] In the Figure 3 dimers, the uncorrected BP curve is always closer to the HF curve than the MP2 curve (in one of the cases, it even lies above the HF curve). Once the correction term is added to the BP energy, the resulting BP-disp curve is clearly closer

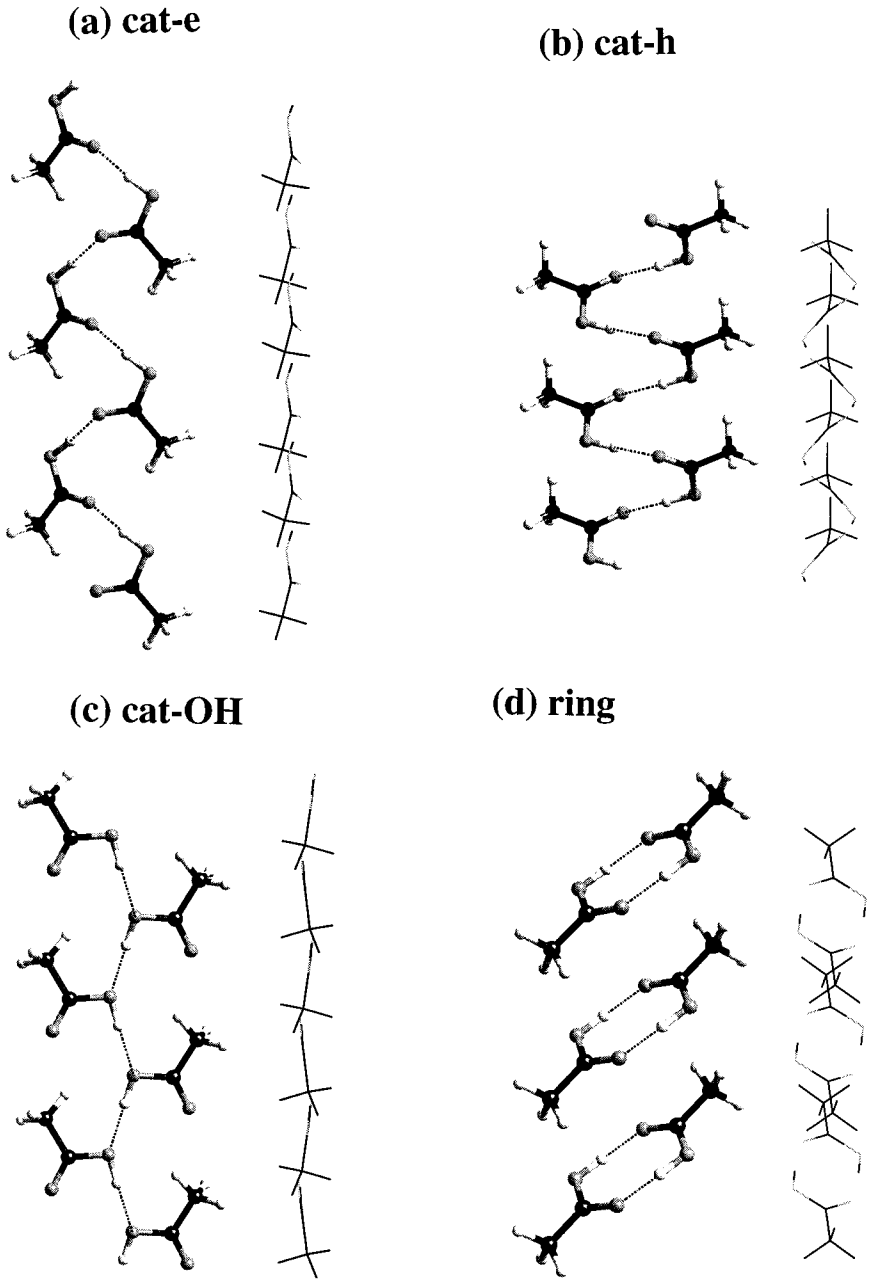

Figure 2. Types of packing motifs found in the most stable UPACK/GROMOS polymorphs: (a) catemer-experimental, (b) catemer-helicoidal, (c) catemer-OH, and (d) ring.

to the MP2 curve. As the HF−MP2 energy difference (the correlation energy) is mostly associated to the dispersion term (note, however, that there are other smaller components associated to the change in the charge distribution of the molecule and polarizability when the correlation is added) and as there is a consensus in the DFT literature on weak interactions that the failure of the currently available DFT functionals on weak complexes is due to the poor description they make of the long-range dispersion,[19] our name "dispersion term" also seems appropriate to the correction term. It is also worth noting that the BP-disp curves presents their minima in the same region as the MP2 curve (the BP curves have their minima at much larger distances), that is, in the region of distances in which the shortest distances are found in the experimental crystal.

Using the curves of Figure 4, one can estimate the impact of including or not including the dispersion term in the computation of the interaction energy of the low-pressure experimental acetic acid crystal. In this crystal, each acetic molecule makes about 10 short contacts of the C−H···OH or C−H···O═C type. By adding BP-MP2 differences on these contacts, one can estimate that the BP computations underestimate the interaction energy of this crystal by 6 about kcal/mol. This underestimation increases if larger distance contacts are also taken into consideration. In any case, the size of this underestimation is on the order of the energy difference between the BP and the experimental interaction energy for that crystal. In fact, the interaction energy of this crystal after adding the dispersion terms is −16.62 kcal/mol, nearly identical to the experimental value for the same crystal. The weight of the dispersion term, −9.30 kcal/mol, clearly demonstrates the net impact on the crystal stability of the estimation of the absolute intermolecular interaction energy.

Interaction Energy of the Most Stable Polymorphs. Once we know what tools we have to use to reproduce the experimental interaction energies using the Car−Parrinello BP ab initio methodology, we can turn our attention into the relative stability

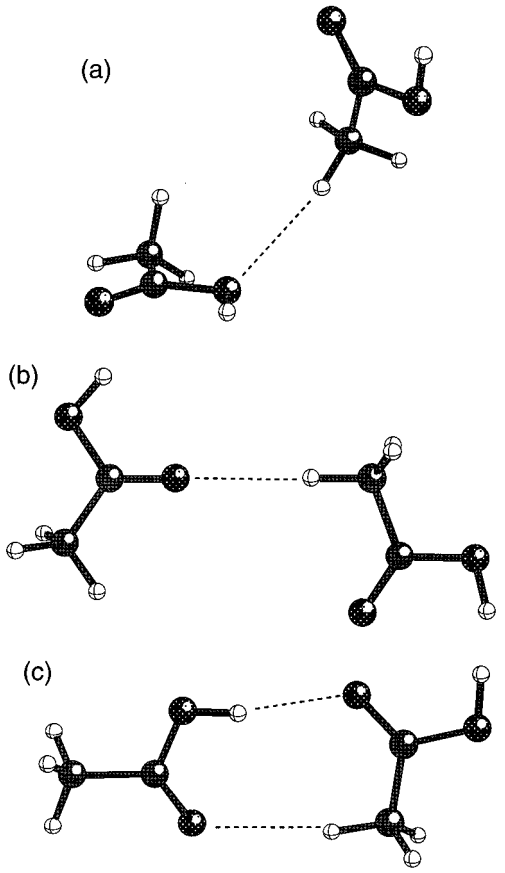

Figure 3. Geometry of the model dimers used to compute the potential energy curves of the C−H···OH, C−H···O═C, and O−H···O═C interactions (models a, b, and c, respectively). They mimic the most common dimer geometries found in the most stable acetic acid polymorphs.

for the UPACK-GROMOS polymorphs of Tables 1 and 2, as computed at the ab initio level. Tables 3 and 4 collect the BP and BP-disp interaction energies computed for the polymorphs in Tables 1 and 2 at the optimum UPACK-GROMOS geometry. The results present the following main points:

(1) all the BP and BP-disp energies lie a lot higher than the energy computed for the experimental crystal (last row of both tables);

(2) the polymorph resembling more closely the experimental crystal, polymorph 13, which was the 15th in stability in the GROMOS computations, is the most stable one in the BP and BP-disp computations;

(3) the size of the dispersion correction, on average −13.05 kcal/mol (with a maximum and minimum values of −12.67 and −13.49 kcal/mol, respectively), is similar in all polymorphs and larger than the BP interaction energy for these polymorphs;

(4) as is graphically shown in Figure 5a, the BP and BP-disp relative stability of the polymorphs is the same for the lowest-energy structures but changes in some of the remaining structures, although the BP and BP-disp interaction energy follows similar overall trends;

(5) the range of variation of the BP and BP-disp interaction energy (6.30 kcal/mol) is much larger than the range of variation of the UPACK/GROMOS interaction energies (0.5 kcal/mol) and does not respect that found in the UPACK/GROMOS computations.

This last point is clearly observed in Figure 5b, where it is also clear that the change in relative stability between the GROMOS and ab initio values is not uniform: many of the most stable polymorphs in GROMOS become highly unstable in the BP-disp case,

There are two other points about the interaction energy which are also of relevance: (a) the positive value of many of the BP interaction energies (indicating that the crystal would sublimate into its gas phase constituting molecules), a fact not present in the BP-disp values, and (b) the difference between the BP or BP-disp value of the most stable UPACK/GROMOS polymorphs and the equivalent values for the low-phase experimental structure. This low stability of the UPACK/GROMOS optimized structures is due to geometrical factors, that is, to the overcompression felt by the molecules within the unit cell predicted by UPACK/GROMOS. This is demonstrated by optimizing the UPACK/GROMOS geometry of the most stable polymorphs at the BP or BP-disp levels (polymorph 13), a process which gives rise, without barrier, to an structure nearly identical to the low-pressure experimental one, with a rapid decrease of the interaction energy (see next section). The geometrical parameters contributing more to such energetic decrease are the cell parameters. Without that relaxation, the molecules are too close to each other and, thus, forced toward regions of their potential energy curve shorter than their minimum (this is clearly seen by comparing intermolecular distances of the two structures in Figure 1 and the curves of Figure 4). As a consequence, their interaction energy decreases.

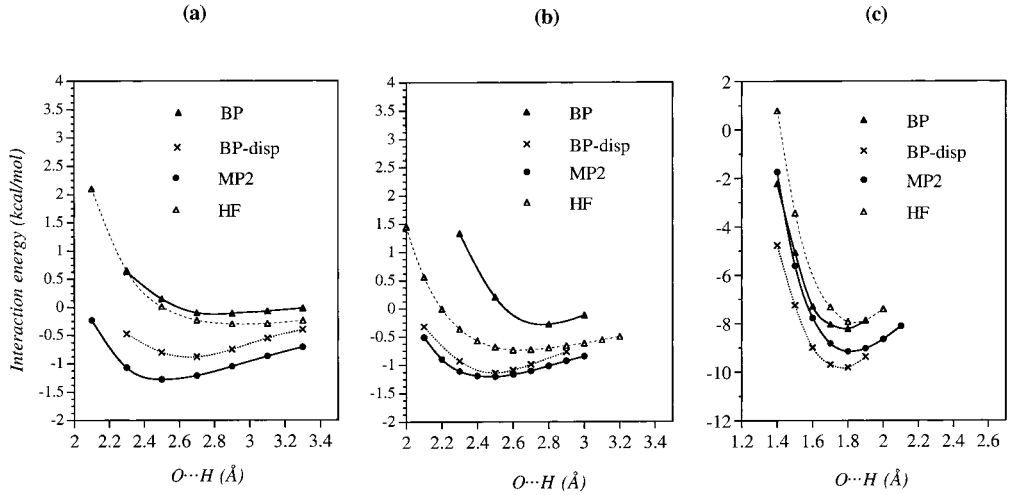

Figure 4. Variation of the potential energy curves with the O···H distance for the dimers of Figure 3, when the O···H is stretched while keeping the relative orientation of the fragments: (a) C−H···OH, (b) C−H···O═C, and (c) O−H···O═C curves. The curves have been computed using the Hartree−Fock (HF), MP2, and BP density functional with and without adding the dispersion term (BP and BP-disp curves, respectively).

TABLE 3: Interaction Energy (in kcal/mol) Computed at the Ab Initio Level for the 30 Structures of the First Subset (Table 1)[a]

number	sp group	motif	*E*(BP)	*E*(disp)	*E*(BP−disp)
13	*Pna*21	cat-e	−1.21	−12.75	−13.96
9	*P*212121	cat-h	−1.01	−12.75	−13.76
14	*P*21	cat-h	−0.91	−12.78	−13.69
50	*P*21/*C*	ring	−0.81	−12.85	−13.66
494	*P*21/*C*	cat-h	−0.71	−12.86	−13.57
116	*P*21/*C*	ring	−0.21	−13.07	−13.28
815	*P*21/*C*	cat-h	−0.01	−12.86	−12.87
31	*P*21/*C*	ring	+0.19	−13.11	−12.92
973	*P*21/*C*	ring	+0.39	−13.43	−13.04
97	*P*212121	cat-e	+0.39	−12.70	−12.31
119	*P*21/C	cat-h	+0.39	−12.81	−12.42
76	*Pna*21	cat-h	+0.49	−13.14	−12.65
118	*P*-1	ring	+0.49	−13.38	−12.89
16	*C*2/*C*	ring	+0.49	−13.12	−12.63
181	*P*21/*C*	cat-h	+0.49	−13.38	−12.89
41	*P*21	cat-e	+0.49	−12.77	−12.28
930	*C*2/*C*	cat-e	+0.59	−12.88	−12.29
34	*P*21/*C*	ring	+0.59	−13.06	−12.47
715	*C*2/*C*	cat-e	+0.69	−13.35	−12.66
6	*Pbca*	cat-e	+0.89	−12.76	−11.87
45	*P*21/*C*	cat-e	+0.89	−13.00	−12.11
4	*Pbca*	cat-e	+1.19	−13.22	−12.03
976	*C*2/*C*	ring	+1.19	−13.49	−12.30
28	*P*212121	cat-e	+1.19	−13.31	−12.12
13′	*C*2/*C*	cat-e	+1.39	−13.05	−11.66
125	*P*-1	ring	+1.49	−13.22	−11.73
362	*P*21/*C*	cat-e	+1.89	−13.16	−11.27
219	*P*21/*C*	ring	+2.09	−13.37	−11.28
216	*P*21/*C*	cat-e	+2.29	−13.25	−10.96
1002	*P*21/*C*	cat-e	+4.19	−12.67	−8.48
Exp.	*Pna*21	cat-e	−7.32	−9.30	−16.62

[a] Each structure is identified by an identification number (first column) identical to that used in ref 6. The space group and packing motif is also given for convenience. For each structure, the interaction energy computed by the direct application of the Becke-Perdew (*E*(BP)) is given, together with the value of the dispersion correction term (*E*(disp), see text for definition) and the *E*(BP−disp), defined as the sum of the previous two components. The crystal geometry is that computed by UPACK/GROMOS.

TABLE 4: Interaction Energy (in kcal/mol) Computed at the Ab Initio Level for the Eight Structures of the Second Subset (Table 2)[a]

number	sp group	motif	*E*(BP)	*E*(disp)	*E*(BP−disp)
13	*Pna*21	cat-e	−1.21	−12.75	−13.96
78	*Pna*21	cat-h	−1.21	−12.12	−13.33
76	*Pna*21	cat-h	+0.49	−13.14	−12.65
47	*Pna*21	cat-h	+0.69	−12.14	−11.45
34	*Pna*21	cat-e	+0.89	−12.85	−11.96
63	*Pna*21	cat-e	+1.39	−12.40	−11.01
182	*Pna*21	cat-OH	+3.59	−12.98	−9.39
79	*Pna*21	cat-OH	+4.89	−13.02	−8.04
exp.	*Pna*21	cat-e	−7.32	−9.30	−16.62

[a] Each structure is identified by an identification number (first column) identical to that used in ref 6. The space group and packing motif is also given for convenience. For each structure, the interaction energy computed by the direct application of the Becke−Perdew (*E*(BP)) is given, together with the value of the dispersion correction term (*E*(disp), see text for definition) and the *E*(BP-disp), defined as the sum of the previous two components. The crystal geometry is that computed by UPACK/GROMOS.

Ab Initio Optimization of the Most Stable Polymorphs. We carried out the geometry optimization of some of the most stable polymorphs in two steps. We first performed an optimization at fixed cell parameters of the relative orientation of the molecules for the following UPACK/GROMOS structures: polymorph 13, the less stable polymorph of Table 3 (polymorph 1002), and for three polymorphs whose stability sits between that for the previous two cases, polymorphs 76, 125, and 362.

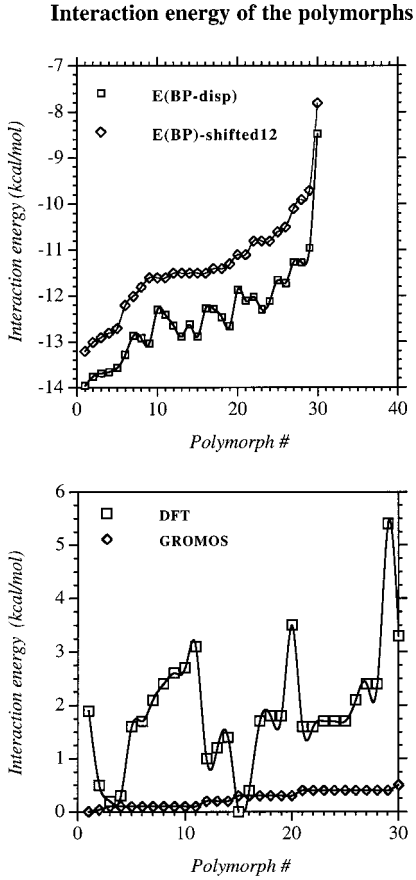

Figure 5. (a) Comparison of the BP and BP-disp interaction energy computed for the Table 1 polymorphs (the BP values have been shifted by a constant −12 kcal/mol value to facilitate the comparison). (b) Comparison of the interaction energy for the most stable UPACK/GROMOS polymorphs computed using the GROMOS potential and the ab initio methodology of this work. The polymorph structure is the optimized UPACK/GROMOS structure.

TABLE 5: Interaction Energy (in kcal/mol) Computed at the Ab Initio Level for the Five Structures Indicated after Optimizing the Geometry of the Crystal, while Fixing the Cell Parameters at the Optimum UPACK/GROMOS Values[a]

number	sp group	motif	*E*(BP)	*E*(disp)	*E*(BP-disp)
13	*Pna*21	cat-e	−1.99	−12.75	−14.74
76	*Pna*21	cat-h	−1.69	−13.14	−14.83
125	*P*-1	ring	−0.09	−13.18	−13.27
362	*P*21/*c*	cat-e	+1.31	−13.16	−11.85
1002	*P*21/*c*	cat-e	+3.01	−12.67	−9.66

[a] Each structure is identified by an identification number (first column) identical to that used in ref 6. The space group and packing motif is also given for convenience. For each structure, the interaction energy computed by the direct application of the Becke−Perdew (*E*(BP)) is given, together with the value of the dispersion correction term (*E*(disp), see text for definition) and the *E*(BP−disp), defined as the sum of the previous two components.

As a result of this partial geometry optimization, all polymorphs increased their stability (Table 5), although in a nonuniform way (see Figure 6), which ranks from 0.78 kcal/mol in polymorph 13, to 2.18 kcal/mol in polymorph 76. However, the interaction energy of the five partially optimized polymorphs is still higher than the BP-disp interaction energy computed for the low-pressure experimental crystal (for instance, polymorph 13 lies still about 5 kcal/mol higher than the experimental crystal).

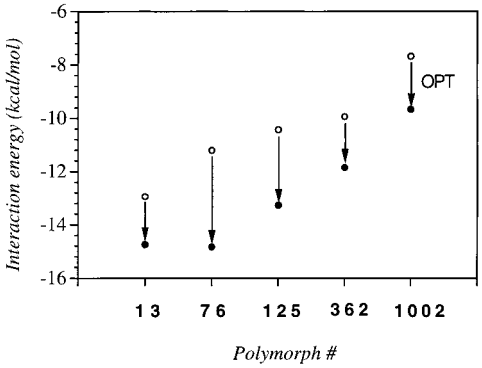

Figure 6. Change in the BP interaction energy for polymorphs 13, 76, 125, 362, and 1002 when their geometry is optimized at the BP level while fixing the cell parameters at their UPACK/GROMOS values.

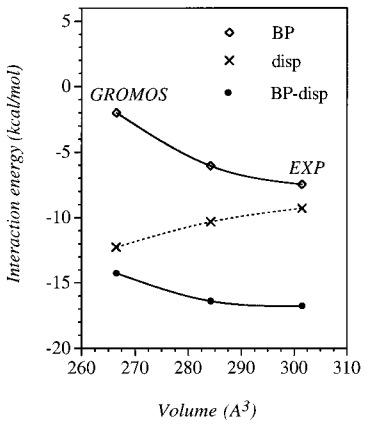

Figure 7. Dependence of the interaction energy of polymorph 13 as the cell parameters are changed toward their experimental values (EXP), starting from the UPACK/GROMOS values (GROMOS).

In light of the previous results, we evaluated in polymorph 13 the impact of optimizing the cell parameters also. The UPACK-GROMOS cell parameters for this polymorph are $a = 14.27$ Å, $b = 3.94$ Å, and $c = 4.74$ Å (all the angles are 90°), while the corresponding experimental parameters are $a = 13.22$ Å, $b = 3.96$ Å, and $c = 5.76$ Å (all angles also are 90°). Consequently, the UPACK-GROMOS unit cell is too large along the *a* direction and too short in the *c* direction, creating the net effect of a decrease in the volume of the UPACK-GROMOS unit cell to 266.5 Å^3 compared to the experimental value (301.5 Å^3). We explored how the BP and BP-disp interaction energy changed as the cell parameters were allowed to go form their UPACK-GROMOS value up to their experimental values (both given above). For such a task, we took an intermediate value between those two sets of parameters, that is, enlarging the *a* value and decreasing *c*, in such a way that the cell volume is exactly half the difference in volume between the UPACK/GROMOS and experimental cells (the exact cell parameters are $a = 13.74$ Å, $b = 3.94$ Å, and $c = 5.25$ Å, all angles being equal to 90°). Then the atom positions of the molecules within this cell were optimized for that fixed cell. The total BP and BP-disp interaction energy obtained after this partial optimization sits between that for the UPACK/GROMOS cell parameters and the experimental cell (see Figure 7), thus indicating that the UPACK/GROMOS cell parameters are not a local minimum and will relax to the experimental values without barrier once they are included in the optimization process. It is interesting to note the similar shape of the energy variation found for the BP and BP-disp curves, despite the fact that the weight of the dispersion term changes a lot with the cell parameters.

The previous results show how the UPACK/GROMOS structure closer to the experimental one relaxes without barrier into the experimental structure when fully optimized at the BP or BP-disp level. However, these computations are equivalent to a 0 K experiment, and the experimental results are at higher temperatures. Therefore, we decided to test the stability of the minimum-energy nature of the BP optimized structure (nearly identical to the experimental structure) by a doing a short-time molecular dynamics study of the experimental structure at the temperature and pressure conditions found in the experimental crystal.

We decided to carry out molecular dynamics (MD) studies of the low-pressure experimental crystal at a temperature below the melting temperature of acetic acid. These MD simulations were done for a total time of 2−3 ps, and the first picosecond was taken as the equilibration period. It is to be noted that first-principles MD for structures of this size are computationally quite demanding. For instance, a 3 ps simulation of one polymorph (roughly the minimum time needed to have an idea of its dynamical behavior) is about three times the cost of the structural optimization for the same system. Thus, it would be computationally prohibitive for us at the present moment to perform a long time MD simulation on all polymorphs of Tables 1−4. However, it is large enough as to have a glimpse at the structural stability and possible phase transitions of the studied polymorph.

A first MD study was done at 250 K and fixed cell parameters, and no change toward another structure was observed. Then the cell parameters were also included in the dynamics. In this case, the average temperature was set to 50 K during the first 1.5 ps, followed by heating to 150 K and continuing the simulation for 1 ps. The analysis of the geometrical parameters for all the points of the dynamics in the second case showed that the cell parameters essentially oscillate around their equilibrium values, differing their averaged values by less than 2% from the experimental values at 133 K. Besides, the averaged density was in very good agreement with the experimental density (1.32 g cm^{-3}). Therefore, the experimental structure did not evolve into another structure during our simulation time. This indicates that the low-pressure experimental structure is a minimum on the ab initio potential energy surface and the energetic barrier for a change toward another type of packing is too high to observe any transition. We have also found that during these simulations the distribution of intermolecular distances follows a Gaussian shape, corresponding to a minimum-energy structure. This is clearly shown in Figure 8 for the distribution of O···H distances along the molecular chains. The CH_3 groups in this dynamics are found to be rather mobile but do not rotate freely, an effect that we attributed to the existence of the stable CH···O interactions.

We also carried out MD simulations at 250 K on polymorph 715, whose structure is that closest to the high-pressure polymorph of the acetic acid.[11] The BP optimized structure of this polymorph is that shown in Figure 9, together with some selected intermolecular distances. Although it has the same packing pattern as the low-pressure experimental crystal, its BP-disp interaction energy (−16.01 kcal/mol) is higher than that for the low-pressure experimental crystal. MD studies, done at the fixed UPACK/GROMOS cell parameters, showed no tendency to transform into another polymorphic structure. However, the wider distribution of the O···H distances (Figure 9) suggests that the cell parameters are not at their optimum ab

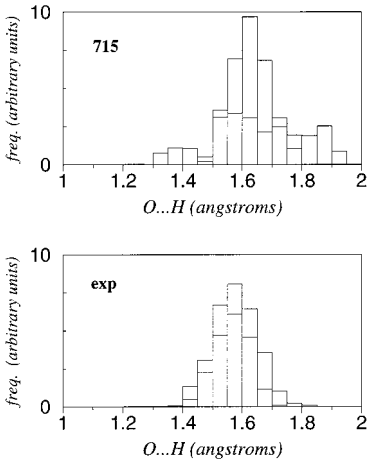

Figure 8. Number of contacts (in arbitrary units) found at a given O···H distances found during the dynamics simulation. The lower graph is for the experimental structure, and the upper graph is for polymorphs 715 at their UPACK/GROMOS optimized cell parameters.

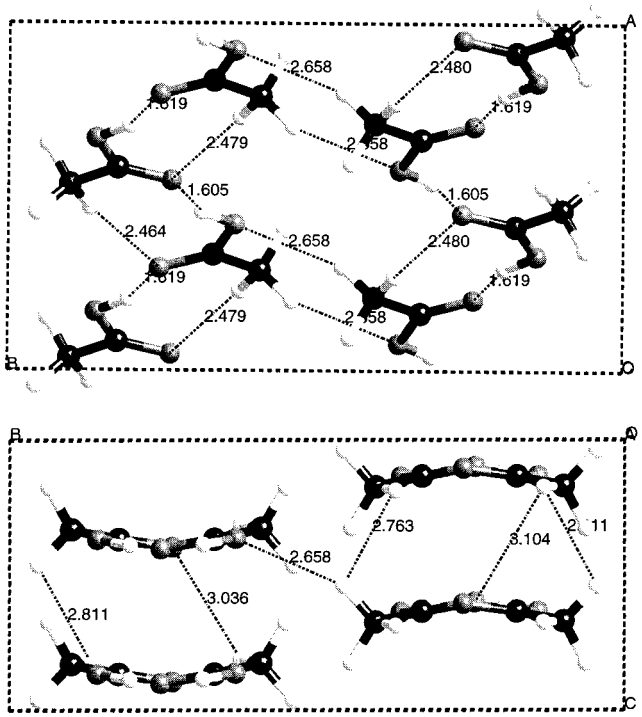

Figure 9. Views of the ab initio optimum-energy structure of polymorph 715 optimized at the fixed UPACK/GROMOS cell parameters.

initio values; the system probably deviates from the minimum-energy dynamical behavior found at the same temperature in the experimental structure to deal with the restriction of the imposed translational symmetry. When the cell parameters were relaxed from their UPACK/GROMOS values toward their experimental values, the interaction energy decreased smoothly and without barrier toward the interaction energy of the experimental high-pressure structure.[27]

Concluding Remarks

Using as a starting point the polymorph crystal structures predicted by UPACK/GROMOS, we have obtained results which show the ability of the ab initio Car−Parrinello BP methodology to reproduce the known experimental information about the structure and relative stability of the polymorphic forms of the acetic acid crystal. The most stable polymorph in these ab initio computations is that reported to have an structure closer to the low-pressure experimental structure, whose energy ranked 15th in the UPACK/GROMOS computations. When the UPACK/GROMOS structure for that polymorph is fully re-optimized at the ab initio level, we find a structure which differs in less than 2% from the experimental one. Geometry optimization at fixed cell parameters is not enough to move the energy of polymorph 13 into the experimental energy range. We have also seen that it is possible to get for these polymorphs interaction energies in the range of the experimental values, if a properly chosen correction term (here called dispersion term) is added to the Becke−Perdew interaction energy. Such a term neither changes the order of relative stability between the most stable polymorphs nor affects the shape of the potential energy surface during geometry optimization of the most stable polymorph. When a short-time ab initio molecular dynamics simulation is done on the low-pressure experimental structure, this structure is found to have minimum energy, and the ab initio average cell parameters differ by less than 2% from the experimental values. No tendency to transform into another packing pattern was detected.

We also carried out a MD study at fixed cell parameters on polymorph 715, the UPACK/GROMOS candidate to the high-pressure energy form of the acetic acid. The crystal relaxed its structure but did not change its packing pattern. In this MD study, we also found a non-Gaussian distribution of the O···H distances, indicating that the crystal is not a minimum-energy structure, probably because the lack of optimization of the cell parameters. When these cell parameters are allowed to relax, the interaction energy smoothly decreases without energy barrier toward the interaction energy of the high-pressure experimental crystal structure.

All the facts considered, we find that atom−atom potentials in conjunction of polymorph predictor programs give qualitatively reasonable structures. However, if accurate results are desired, one has to refine these structures by better methods (like ab initio computations).

Acknowledgment. This work was supported by the CICYT (Project PB98-1166-C02-02) and CIRIT (1999SGR-00046) and also by a grant of computer time provided by CESCA-CEPBA and the University of Barcelona. C.R. acknowledges "Ministerio de Educación y Cultura" for her Contract "Programa de Incorporación de Doctores y Tecnólogos". We than Dr. W. T. M. Mooij for sending us the Supporting Information of its article and for his help in decoding these structures.

References and Notes

(1) Bernstein, J.; Davey, R. J.; Henck, J.-O. *Angew. Chem., Int. Ed. Engl.* **1999**, *38*, 3440. Dunitz, J.; Bernstein, J. *Acc. Chem. Res.* **1995**, *28*, 193. Dunitz, J. *Acta Crystallogr.* **1995**, *B51*, 619.

(2) Kinoshita, M. *Jpn. J. Appl. Phys.* **1994**, *33*, 5718. Miller, J. S.; Epstein, A. J. *Angew. Chem., Int. Ed. Engl.* **1994**, *33*, 385.

(3) (a) Ishiguro, T.; Yamaji, K. *Organic Superconductors*; Springer-Verlag: Berlin, 1990. (b) Williams, J. M.; Ferraro, J. R.; Thorn, R. J.; Carlson, K. D.; Geiser, U.; Wang, H. H.; Kini, A. M.; Whangbo, M.-H. *Organic Superconductors*; Prentice Hall: Englewood Cliffs, New Jersey, 1992.

(4) Gavezzotti, A. *Acc. Chem. Res.* **1994**, *27*, 309. See also: *Crystal Engineering: from Molecules and Crystals to Materials*; Braga, D., Grepioni, F., Orpen, A. G., Eds.; Kluwer: Dordretch, 1999.

(5) (a) Gavezzotti, A. *J. Am. Chem. Soc.* **1991**, *113*, 4622. (b) Gdanitz, R. J. In *Theoretical aspects of computer modeling;* Gavezzotti, A., Ed.; John Wiley: Chichester, 1997. (c) Perlstein, J. *J. Am. Chem. Soc.* **1992**, *114*, 1955. (d) Holden, J. R.; Du, Z.; Ammon, H. L. *J. Comput. Chem.* **1993**, *14*, 422. (e) van Eijck, B. P.; Mooij, W. T. M.; Kroon, J. *Acta Crystallogr.* **1995**, *B51*, 99. (f) Chaka, A. M.; Zaniewski, R.; Youngs, W.; Tessier, C.; Klopman, G.; *Acta Crystallogr.* **1996**, *B52*, 165. (g) Schmidt,

M. U.; Englert, U. *J. Chem. Soc., Dalton Trans.* **1996**, 2077. Hofmann, D. W. M.; Lengauer, T.; *Acta Crystallogr.* **1997**, *A53*, 225. Vermer, P.; Leusen, F. J. J.; *Rev. Comput. Chem.* **1998**, *12*, 327.

(6) For an example of polymorph prediction giving many feasible energetic forms, see the predictions for the acetic acid carried out in: (a) Mooij, W. T. M.; van Eijck, B. P.; Price, S. L.; Vermer, P.; Kroon, J. *J. Comput. Chem.* **1998**, *19*, 459. (b) Payne, R. S.; Roberts, R. J.; Rowe, R. C.; Docherty, R. *J. Comput. Chem.* **1998**, *19*, 1.

(7) See, for instance: Payne, R. S.; Rowe, R. C.; Roberts, R. J.; Charlton, M. H.; Docherty, R. J. *J. Comput. Chem.* **1999**, *20*, 262.

(8) Filippini, G.; Gavezzotti, A.; Novoa, J. J. *Acta Crystallogr.* **1999**, *B55*, 543.

(9) (a) Mooij, W. T. M.; van Duijneveldt, F. B.; van Duijneveldt-van de Rijdt, J. G. C. M.; Eijck, B. P. *J. Phys. Chem. A* **1999**, *103*, 9872. (b) Beyer, T.; Price, S. L. *J. Phys. Chem. B* **2000**, *104*, 2647.

(10) (a) Leiserowitz, L. *Acta Crystallogr.* **1976**, *B32*, 775. (b) Allen, F. H.; Motherwell, W. D. S.; Raitby, P. R.; Shields, G. P.; Taylor, R. *New. J. Chem.* **1999**, 25.

(11) Allan, D. R.; Clark, S. J. *Phys. Rev. B* **1999**, *60*, 6328.

(12) (a) Hagler, A. T.; Dauber, P.; Lifson, S. *J. Am. Chem. Soc.* **1979**, *101*, 5131. (b) Turi, L.; Dannenberg, J. J. *J. Am. Chem. Soc.* **1994**, *116*, 8714. (c) Gavezzotti, A. *Chem. Eur. J.* **1999**, *5*, 567. (d) Nakabayashi, T.; Kosugi, K.; Nishi, N. *J. Phys. Chem. A* **1999**, *103*, 8595.

(13) (a) Becke, A. D. *J. Chem. Phys.* **1986**, *84*, 4524. (b) Perdew, J. P. *Phys. Rev. B* **1986**, *33*, 8822.

(14) (a) Car, R.; Parrinello, M. *Phys. Rev. Lett.* **1985**, *55*, 2471. (b) Galli, G.; Parrinello M. In *Computer Simulation in Materials Science*; Pontikis, V., Meyer, M., Eds.; Kluwer: Dordrecht, 1991.

(15) Hutter, J. *CPMD-3.0*; Max-Plank-Institut für Festköerperforchung: Stuttgart, Germany, 1998.

(16) Troullier, N.; Martins, J. L. *Phys. Rev.* **1991**, *B43*, 1993.

(17) The BSSE was coreected using the full counterpoise method of Boys−Bernardi. The BSSE error distorts the interaction energy computed for hydrogen bonded complexes, but the counterpoise method provides BSSE-corrected interaction energy for hydrogen bonded complexes, which are more stable with respect to the basis set employed and approach the available experimental values, provided that a minimum quality is reached on the basis. See: (a) Boys, S. F.; Bernardi, F. *Mol. Phys.* **1970**, *19*, 553. (b) van Duijneveldt, F. B.; van Duijneveldt-van der Rijdt, J. G. C. M.; van Lenthe, J. H. *Chem. Rev.* **1994**, *94*, 1873. (c) Novoa, J. J.; Planas, M.; Rovira, M. C. *Chem. Phys. Lett.* **1996**, *251*, 33. (d) Novoa, J. J.; Planas, M. *Chem. Phys. Lett.* **1998**, *285*, 186.

(18) Saunders, V. R.; Dovesi, R.; Roetti, C.; Causa, M.; Harrison, N. M.; Orlando, R.; Zicovich-Wilson, C. M. *CRYSTAL98 User's Manual*; University of Torino: Torino, 1998.

(19) See, for instance: (a) Kristyan, S.; Pulay, P. *Chem. Phys. Lett.* **1975**, *229*, 175. (b) Sponer, J.; Leszcynski, J.; Hobza, P. *J. Comput. Chem.* **1996**, *17*, 841. (c) Novoa, J. J., Sosa, C. *J. Phys. Chem.* **1995**, *99*, 15837.

(20) Bernasconi, M.; Chiarotti, G. L.; Focher, P.; Parrinello, M.; Tosatti, E. *Phys. Rev. Lett.* **1996**, *76*, 2081.

(21) Meijer, E. J.; Sprik, M. *J. Chem. Phys.* **1996**, *105*, 8684.

(22) Frisch, M. J.; Trucks, G. W.; Schlegel, H. B.; Scuseria, G. E.; Robb, M. A.; Cheeseman, J. R.; Zakrzewski, V. G.; Montgomery, J. A., Jr.; Stratmann, R. E.; Burant, J. C.; Dapprich, S.; Millam, J. M.; Daniels, A. D.; Kudin, K. N.; Strain, M. C.; Farkas, O.; Tomasi, J.; Barone, V.; Cossi, M.; Cammi, R.; Mennucci, B.; Pomelli, C.; Adamo, C.; Clifford, S.; Ochterski, J.; Petersson, G. A.; Ayala, P. Y.; Cui, Q.; Morokuma, K.; Malick, D. K.; Rabuck, A. D.; Raghavachari, K.; Foresman, J. B.; Cioslowski, J.; Ortiz, J. V.; Stefanov, B. B.; Liu, G.; Liashenko, A.; Piskorz, P.; Komaromi, I.; Gomperts, R.; Martin, R. L.; Fox, D. J.; Keith, T.; Al-Laham, M. A.; Peng, C. Y.; Nanayakkara, A.; Gonzalez, C.; Challacombe, M.; Gill, P. M. W.; Johnson, B. G.; Chen, W.; Wong, M. W.; Andres, J. L.; Head-Gordon, M.; Replogle, E. S.; Pople, J. A. *Gaussian 98*, revision A.7; Gaussian, Inc.: Pittsburgh, PA, 1998.

(23) (a) van Ginkel C. H. D. C.; Calis, G. H. M.; Timmermans, C. W.; de Kruif, C. G.; Oonk, H. A. J. *J. Chem. Thermodyn.* **1978**, *10*, 1083. (b) Chickos, J. S. *Molecular Structure and Energetics*; Liebman, J. F., Greenberg, A., Eds.; VCH: New York, 1987; Vol. 2.

(24) (a) Novoa, J. J.; Deumal, M. *Mol. Cryst. Liq. Cryst.* **1997**, *305*, 143. (b) Deumal, M.; Cirujeda, J.; Veciana, J.; Kinoshita, M.; Hosokoshi, Y.; Novoa, J. J. *Chem. Phys. Lett.* **1997**, *265*, 190. (c) Novoa, J. J. In *Implications of Molecular and Materials Structure for New Technologies*; Allen, F., Howard, J., Shields, G. P., Eds.; Kluwer Academic Publishers: Dordrecht, 1999.

(25) (a) Etter, M. C. *Acc. Chem. Res.* **1990**, *23*, 120. (b) Bernstein, J.; Davis, R. E.; Shimoni, L.; Chang, N.-L. *Angew. Chem., Int. Ed. Engl.* **1995**, *34*, 1555.

(26) See, for instance: (a) Novoa, J. J.; Tarron, B.; Whangbo, M.-H.; Williams, J. M. *J. Chem. Phys.* **1991**, *95*, 5179. (b) Rovira, M. C.; Novoa, J. J.; Whangbo, M.-H.; Williams, J. M. *Chem. Phys.* **1995**, *200*, 319. (c) Novoa, J. J.; Planas, M.; Rovira, M. C. *Chem. Phys. Lett.* **1996**, *251*, 33. (d) Novoa, J. J.; Mota, F. *Chem. Phys. Lett.* **1997**, *266*, 23.

(27) Details of these computations are given in: Ronra, C.; Novoa, J. J., *J. Chem. Phys.* **2000**, *113*, 9208.